JOURNAL OF CATALYSIS 138, 164–178 (1992)

Benzene Ethylation and Cumene Dealkylation over Nickel-Loaded Y Zeolites

BRENDAN COUGHLAN AND MARK A. KEANE[1]

Physical Chemistry Laboratories, University College, Galway, Ireland

Received December 12, 1991; revised April 27, 1992

The alkylation and dealkylation activities of a range of nickel-loaded Y zeolites, prepared by ion exchange and impregnation, have been measured and correlated to the surface Brønsted acidity. The effect on the level of protonic activity of varying the alkali metal co-cation (Li^+, Na^+, K^+, Rb^+, or Cs^+) and the inclusion of Ce^{3+} ions is discussed. With a vew to optimising catalytic efficiency, a number of parameters were considered: these were catalyst precursor reduction temperature, catalyst precalcination, reaction temperature, acid poisoning by pyridine adsorption, coke deposition, and catalyst regeneration. The presence of nickel metal on the support served to enhance the ethylation and cracking activities by converting coke precursors. In the case of benzene ethylation, diethylbenzenes were formed over the most active samples; the relative distributions of the *ortho*-, *para*-, and *meta*-isomers are reported. For comparative purposes, data on benzene ethylation over nickel-impregnated silica and alumina catalysts are also presented.

INTRODUCTION

The search for correlations between the acidic and catalytic properties of acidic oxides remains ongoing. The introduction of zeolites as acidic crystalline aluminosilicate supports has provoked further interest in this field. In attempting to refine the description of active sites, it is now evident that the well-defined zeolite structure does not allow for a simple solution to the problem (*1*). Indeed, Barthomeuf (*2*) has proposed that the acidic behaviour of zeolites is governed by properties which are independent of crystallographic structure and are more relevant to the model of acidic solutions. In effect, zeolites may be considered as solids behaving, more or less, like protonic polyacids in solution. In contrast to other solid acids, the zeolitic protons (as in solutions) are free to move inside and through the zeolite framework while remaining in close contact with the structural atoms.

The ethylation of benzene with ethanol has proved to be particularly useful for probing the catalytic properties of acidic zeolites (*3, 4*). The high electron density associated with the benzene ring renders it susceptible to electrophilic attack by positive ion species or by the positive end of a dipole or induced dipole (*5*). It is now generally accepted that alkylation reactions proceed via a carbocation intermediate (*1*). Both kinetic and mechanistic studies support a Rideal-type mechanism (*5–7*) in which the alkylating agent, which is strongly adsorbed at an acid site, reacts with a free or weakly adsorbed benzene molecule in the rate-determining step. In the case of zeolite supports, Brønsted sites (*8*), Lewis sites (*9*), and the charge-balancing cations (*10*) have all been proposed as active centres for promoting alkylation reactions. Becker *et al.* (*11*) observed a maximum in ethylation activity at a catalyst precursor activation temperature of 723 K. Catalytic activity and substrate selectivity have been related to

[1] To whom correspondence should be addressed. Present address: Department of Chemistry and Biochemistry, University of Guelph, Guelph, Ontario N1G 2W1, Canada.

0021-9517/92 $5.00

the stability of the catalytic intermediates (*1*). A high selectivity towards *para*-alkylation has been observed for catalysis over Y zeolites (*6, 12*). The alkylation of the benzene ring and side chain(s) is known to proceed on acidic and basic sites, respectively (*13, 14*). Lithium-exchanged zeolite X has been shown to catalyse only ring alkylation (*13–15*), whereas KX, RbX, and CsX selectively catalysed side-chain alkylation (*13, 15–17*). The sodium-based catalyst, however, has been considered by some workers to promote side-chain alkylation (*13, 16*) and by others to catalyze aromatic aklylation (*14, 18*). Regardless, the overall alkylation activity has been reported to decrease in the order (*17*) NaX > KX > CsX.

Cumene dealkylation to benzene and propylene has been used as a test of the cracking activity of acid catalysts (*1, 19–23*). The reaction can be viewed as a reverse alkylation and is generally rationalized in terms of proton attack at an aromatic carbon atom with displacement of the side-chain as a carbonium ion (*1, 19, 20*). Free radical cracking at the exchanged cations also produces styrene and α-methylstyrene at temperatures in excess of 798 K (*1, 20*). Cumene conversions at low reactant partial pressures and at temperatures less than 773 K resulted in the exclusive formation of benzene and propylene (*21*). Alkali metal ion-exchanged Y zeolites have exhibited much lower cracking activities (*22*) compared to the transition metal ion-exchanged forms (*23*). Dealkylation activity has been shown to decrease as a result of coke formation with propylene acting as a coke precursor (*22*).

The alkylation and cracking properties of crystalline aluminosilicates have generally been correlated solely to the acidic function. However, catalytic dual functionality is used extensively in commercial processes such as hydrocracking where the presence of metal "poisons" often play an important role in establishing selectivity factors. With few exceptions, the majority of catalytic studies have been concerned with sodium-based zeolites. To date, ethylation and cracking activity data for hydrogen-reduced nickel Y zeolites, enriched to various levels with different alkali metal cations, have not been documented. In a previous study conducted in this laboratory (*24*), the surface Brønsted acidity generated on the reduction of a range of NiY zeolites was characterized using infrared spectroscopy and Hammett indicators. In this paper, the influence of varying the alkali metal co-cation on the level of benzene ethylation and cumene dealkylation over reduced nickel zeolites is examined and compared with the activities observed over nickel-impregnated silica and alumina.

EXPERIMENTAL

Catalyst Preparation and Activation

The starting or parent zeolite was Linde molecular sieve LSZ-52 which can be represented by the molecular formula $Na_{58}(AlO_2)_{58}(SiO_2)_{134}(H_2O)_{260}$. The alumina (70–230 mesh) and silica (30–120 mesh) supports were supplied by Labkem Ltd. and BDH, respectively. KY and LiY (100% exchange) and RbNaY and CsNaY (ca. 68% exchange) were prepared by exchanging out the parent Na^+ ions. A known weight of NaY, usually 250 g, was refluxed with 400 cm^3 of 1 mol dm^{-3} solutions of $LiNO_3$, KNO_3, RbCl, and CsCl for 24 h, after which the zeolite was vacuum filtered and thoroughly washed with hot deionised water to remove the occluded salt; the zeolite was then air dried at 383 ± 3 K for a further 24 h. The partially exchanged samples, i.e., Li,K,Rb,Cs/NaY, were exchanged an additional nine times and stored over saturated NH_4Cl solutions. A fully exchanged NH_4Y zeolite was prepared by refluxing 250 g of NaY with ca. 400 cm^3 of a 0.5 mol dm^{-3} solution of NH_4NO_3 over a period of 3 days, filtering and drying as before; after 10 such treatments complete exchange was achieved and no residual Na^+ ions were detected by atomic absorption spectrophotometry. In a similar fashion, CeNaY (ca. 68% exchange) and CeKY (ca. 74% exchange) samples were prepared by refluxing

250-g batches of NaY and KY with 0.5 mol dm^{-3} aqueous RbCl and CsCl solutions. Nickel-exchanged samples were prepared by taking 100 g of NaY, LiY, KY, RbNaY, CsNaY, NH_4Y, CeNaY, or CeKY and refluxing with a 400 cm^3 $Ni(NO_3)_2$ solution for 24 h. The pH of the NaY/deionized water suspension was 9.5. It has been reported in the literature (*25*) that many transition metal salt solutions are sufficiently acidic to cause structural breakdown of the zeolite host. Consequently, in this study, dilute nickel nitrate solutions (<0.1 mol dm^{-3}) were used in which the pH of the zeolite/nitrate suspensions was in the range 6–7.5. Under these conditions, a single exchange cycle resulted in a maximum exchange of ca. 7 Ni^{2+}/U.C., i.e., seven nickel cations per unit cell; repeated exchanges were necessary in order to prepare catalysts with higher loadings. Quantitative impregnation of the NaY, LiY, KY, RbNaY, CsNaY, alumina, and silica supports was achieved with constant volumes of $Ni(NO_3)_2$ solutions by vacuum rotary evaporation to incipient wetness. The concentration of the nickel salt was chosen to yield the desired metal content. Atomic absorption (Ni^{2+} concentration) and flame emission (Na^+, Li^+, K^+, Rb^+, and Cs^+ concentrations) techniques, using a Perkin–Elmer 360 spectrophotometer, were employed to determine the cation content to within ±2%. From the measured ion concentrations, the precise mass of zeolite sample and the number of unit cells per gram of parent zeolite, the number of exchanged cations per unit cell was determined. Thermal analyses were also conducted on all the prepared samples using a Perkin–Elmer thermobalance operating in the TG mode to measure the percentage (by weight) water loss as a function of temperature. The ion-exchanged catalysts are labelled according to the percentage exchange of the indigenous alkali metal ions, e.g., NiKY-23.5 exhibits a 23.5% exchange of the original potassium content, which corresponds to a nickel cation content of 6.8 Ni^{2+}/U.C.

The hydrated catalyst precursors were pelletized without binder under a pressure of 4000 kg cm^{-2} and sieved in the mesh range 1.18–1.70 mm. The zeolite pellets were activated by either heating (at 200 ± 2 Kh^{-1}) in a 120 cm^3 min^{-1} stream of purified nitrogen (N_2-treatment) or hydrogen (reduction) to a final temperature of 723 ± 1 K, which was maintained for 18 h. The activated catalysts were then cooled in nitrogen to the desired reaction temperature. The degree of reduction of the exchangeable Ni^{2+} cations was measured by iodometric titrametric and atomic absorption techniques which have been fully described in a previous paper (*26*). The nature of the supported metal phase has also been comprehensively characterized by XRD line broadening and electron microscopy as outlined elsewhere (*27*). X-ray diffraction and infrared spectroscopy were used to monitor the crystallinity of the samples (*27*); the infrared band at 395 cm^{-1} has been shown to be very sensitive to changes in crystallinity (*28*).

Catalytic Procedure

The catalytic reactor was constructed from a Pyrex glass tube 50 cm in length and having an internal diameter of 3 cm. The tube was indented ca. 30 cm from the top in order to provide a means of support for a plug of glass wool on which lay the catalyst pellets. The catalyst bed was further supported between two layers of glass beads and a thin layer of boiling chips. This ensured that the reactants reached the reaction temperature before contacting the catalyst surface. The hydrocarbon reactants were fed into the reactor from a precision motor driven syringe which had been carefully calibrated before use by monitoring the volume of reactant(s) delivered in a given time interval at different motor settings. Exit from the reactor was through a B10 cone and the products were collected in a trap immersed in liquid nitrogen. The carrier gas escaped from the collector and subsequently passed through a bubble flow meter which was used to monitor the gas flow rate. Treatment of

the reduced zeolites with pyridine, to poison the surface Brønsted acid sites, was achieved by passing a steady 5 $cm^3 h^{-1}$ flow of pyridine through the activated zeolite bed at 473 K for 30 min. The catalyst was then flushed in a 120 $cm^3 min^{-1}$ stream of purified N_2 for 1 h and the temperature raised to the desired reaction temperature with a further 3 h N_2 purge prior to catalysis. Oxidative regeneration of the deactivated samples was carried out by heating (at 50 K h^{-1}) the zeolite pellets *in situ* in a 120 $cm^3 min^{-1}$ stream of purified oxygen to a final temperature of 723 ± 1 K, which was maintained for 1 h. The catalysts were then thoroughly purged in a 160 $cm^3 min^{-1}$ flow of N_2 and re-reduced in H_2 as before for 18 h; the temperature was then lowered (in N_2) to the desired reaction temperature. The catalytic reactor and procedure are described in greater detail elsewhere (*29*).

For comparative purposes, it was decided to examine the level of protonic activity under conditions where the maximum number of Brønsted acid sites are present. To this end, a sample of NH_4Y was heated in a 120 $cm^3 min^{-1}$ stream of purified nitrogen to a final temperature of 723 ± 2 K, which was maintained for 18 h; this heat treatment has been shown (*24*) to result in the siting of roughly equal numbers (ca. 29 H^+/U.C.) of protons in the large and small zeolite cages. The techniques used to characterize the catalyst acidity are described in an earlier paper (*24*). In the case of the ethylation reactions, the benzene : ethanol molar ratio was maintained at 3 : 1 and 5 : 1 for the calcined and reduced samples, respectively. The benzene/ethanol feed was delivered at a constant rate of 5 $cm^3 h^{-1}$ in a 120 $cm^3 min^{-1}$ stream of nitrogen. In the case of the cumene reaction, the *W/F* value (weight of hydrated zeolite divided by the flow rate of cumene) was 83.3 g mol^{-1} h and N_2 (120 $cm^3 min^{-1}$) was again the carrier gas.

Product analysis was carried out on the liquid samples, collected in a liquid-nitrogen trap, using a Pye Unicam GCV chromatograph with a flame-ionization detector; the chromatograph was used in conjunction with a Shimadzu Chromatopac C-R3A data processor. The products of the reaction were identified by comparison of the retention times with those of known standards. Analysis of the reaction products was made using a 5% Bentone/5% di-isodecylphthalate on Chromosorb W chromatography column with a carrier gas (N_2) flow rate of 25 $cm^3 min^{-1}$ and column temperature at 348 ± 1 K. The overall level of ethylation (or dealkylation) was converted to percentage mole conversion using a 25-point calibration plot; a quadratic equation was used to fit these data to better than ±1%. Percentage mole conversion after 6 h on stream was used as a point of comparison of different catalysts operating under the same reaction conditions. All the aromatic hydrocarbons (purchased from BDH Chemicals Ltd.) used in this study were of AnalaR grade and were further dried by standard methods (*30*) and stored over sodium wire.

RESULTS AND DISCUSSION

The chemical compositions of the ion exchanged zeolites are given in Table 1. Sample crystallinity was maintained, before and after catalysis, for each of the tabulated samples.

Ethylation of Benzene

In this study, benzene ethylation over the range of calcined and reduced samples considered only yielded ethylbenzene (EB) and *ortho-*, *para-*, and *meta*-diethylbenzenes (DEB) in the product mixture. The formation of butylbenzene, reported when ethylene was used as the alkylating agent (*1*), or the generation of polysubstituted products (*3, 4, 6*) was not detected under the stated experimental conditions. Although this work is primarily concerned with the ethylation of benzene over reduced nickel catalysts, the level of benzene conversion over the N_2-treated, oxidised catalysts was also considered. The N_2-treated alkali metal and nickel ion-exchanged catalysts exhibited a minor degree of ethylation activity which

TABLE 1

Chemical Composition of the Nickel-Loaded Zeolites Prepared by Ion Exchange

Zeolite sample	AM^+/U.C.[a]	Ni^{2+}/U.C.	H^+/U.C.	Water content (w/w%)
NaY	58.0	—	—	25.1
NiNaY- 6.8	53.7	2.0	0.3	25.3
NiNaY-15.8	48.8	4.6	—	26.5
NiNaY-22.8	44.0	6.6	0.8	26.6
NiNaY-27.8	40.9	8.1	0.9	26.8
NiNaY-35.7	36.0	10.4	1.2	27.6
NiNaY-48.8	30.0	14.1	—	28.6
NiNaY-63.1	22.3	18.3	—	29.1
NiNaY-78.6	14.6	22.8	—	29.5
NiNaY-90.1	6.9	26.1	—	30.0
KY	58.0	—	—	22.4
NiKY-26.9	42.4	7.8	—	24.2
NiKY-35.6	36.9	10.3	0.5	24.8
NiKY-44.7	31.9	13.0	0.1	25.5
NiKY-49.1	29.8	14.2	—	26.4
NiKY-57.5	24.8	16.7	—	27.3
NiKY-62.5	22.3	18.1	—	27.6
NiKY-73.8	16.3	21.4	—	28.0
NiKY-82.0	13.1	23.8	—	28.4
NiKY-86.6	8.4	25.1	—	29.3
LiY	58.0	—	—	27.8
NiLiY- 8.8	52.3	2.6	0.5	27.9
NiLiY-21.2	44.6	6.2	1.1	28.2
NiLiY-43.1	32.0	12.4	1.2	28.8
NiLiY-63.7	20.7	18.5	0.3	29.3
NiLiY-80.6	14.2	23.4	—	29.9
RbNaY	40.2[b]	—	—	20.4
NiRbNaY-27.3	24.3	7.9	0.2	23.0
NiRbNaY-35.1	19.8	10.2	—	24.2
NiRbNaY-47.4	15.2	13.7	—	25.9
NiRbNaY-59.1	10.3	17.1	—	27.4
CsNaY	39.8[b]	—	—	7.8
NiCsNaY-31.1	20.7	9.0	—	14.9
NiCsNaY-44.3	13.6	12.8	—	16.6
NiCsNaY-54.8	11.2	15.9	—	19.4
NH_4Y	—	—	58.0	24.3
$NiNH_4Y$- 8.5	—	2.5	53.0	24.3
$NiNH_4Y$-20.7	—	6.0	46.0	25.5
$NiNH_4Y$-52.2	—	15.1	27.7	27.6
$NiNH_4Y$-69.1	—	20.0	17.9	28.1

[a] $AM^+ = Li^+, Na^+, K^+, Rb^+$, or Cs^+.
[b] Number of Rb^+ or Cs^+/U.C.

TABLE 2

Correlation between the Level of Ethylbenzene Formation and the Surface Acidity of a Range of N_2-Treated Zeolites: $T_{reaction}$ = 573 K; Benzene : Ethanol = 3 : 1

Zeolite sample	Acid strength[a] (mmol *n*-butylamine $g_{zeolite}^{-1}$)	Mol% ethylbenzene (6 h on stream)
HY	1.18	21.4
CeNaY-68.0	0.58	16.9
CeKy-74.2	0.49	15.3
LiY	0.08	2.1
NaY	0.03	1.6
KY	—	1.1
RbNaY	—	0.9
CsNaY	—	0.3
NiLiY-21.2	0.10	3.0
NiLiY-63.7	0.19	4.3
NiNaY-22.8	0.05	2.1
NiNaY-63.1	0.10	2.9
NiKY-23.5	0.03	1.4
NiKY-62.5	0.09	2.3
NiRbNaY-27.3	—	1.0
NiRbNaY-59.1	0.06	1.8
NiCsNaY-22.0	—	0.7
NiCsNaY-54.8	0.06	1.3

[a] From Hammett indicator studies (*24*): H_0 = 2.8.

was much lower than that associated with the more acidic HY, CeNaY, and CeKY samples (see Table 2). Indeed, the rank of catalytic activity, CsNaY < RbNaY < KY < NaY < LiY < NiY < CeKY < CeNaY < HY, is consistent with the order of acid strength deduced from earlier Hammett indicator studies (*24*) on the same catalysts. The surface acidity and, hence, the protonic activity of these catalysts is determined by the magnitude of the zeolitic electrostatic field.

The levels of Ni^{2+} reduction (*26*) and the associated Brønsted acidity, which is in the form of protons generated during the reduction step which attach to the lattice oxygens to form framework hydroxyls (*24*), have both been shown to increase with increasing reduction temperature. This is in turn accompanied by an increase in the degree of benzene ethylation (see Fig. 1). Under these reduction conditions there were no detectable Lewis acid sites (*24, 31*); ethylation activity must then be related to the surface Brønsted acidity, in agreement with the findings of other workers (*8, 11, 12*). The extent of benzene ethylation also increased with increasing reaction temperature in the range 473–623 K (see Fig. 2a). This is in complete contrast to the catalytic hydrogenation of benzene and toluene over the same catalysts (*29, 32–34*), where maxima in cyclohexane and methylcyclohexane formation were observed at reaction temperatures lower than 473 K. In contrast to the hydrogenation reaction which we have described in terms of a modified Langmuir–Hinshelwood-type model (*34*), the alkylation of benzene with ethanol is known to proceed via a Rideal-type mechanism (*5–7*) involving the adsorption of ethanol on a hydroxyl group to form an intermediate carbonium ion species which is then attacked in the rate-determining step by a free or weakly adsorbed aromatic species. Benzene has been shown to interact strongly with the unreduced divalent nickel and the indigenous alkali metal cations located in the accessible supercages, the extent of the interaction decreasing markedly at temperatures in excess of 473 K (*35*). As benzene reacts from the vapour phase in the case of the ethylation reaction,

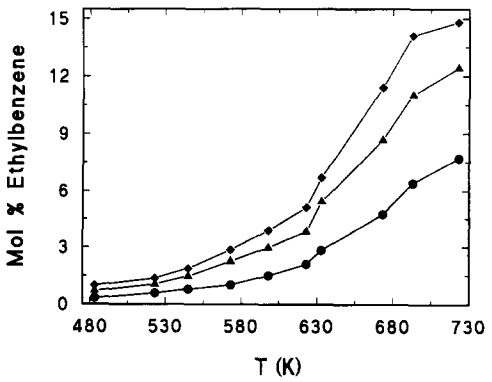

FIG. 1. Mol% conversion of benzene to ethylbenzene (after 6 h on stream at 573 K) over NiLiY-63.7 (◆), NiNaY-63.1 (▲), and NiKY-62.5 (●) as a function of catalyst precursor reduction temperature.

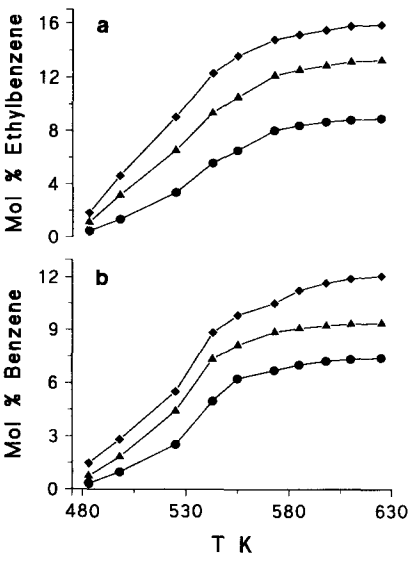

FIG. 2. Mol% conversion of (a) benzene to ethylbenzene and (b) cumene to benzene (after 6 h on stream at 573 K) as a function of reaction temperature over samples of hydrogen-reduced NiLiY-63.7 (♦), NiNaY-63.1 (▲), and NiKY-62.5 (●).

the specific adsorption behaviour reported for the hydrogenaton systems (*29, 32—35*) is not apparent during ethylation. However, the shapes of the conversion vs. temperature profiles, shown in Fig. 2a, are characteristic of a reaction system where the overall activity is diffusion controlled at higher reaction temperatures. In the absence of any temperature related adsorption considerations, the flattening of the profiles over the temperature range 573–623 K must be due to a deactivation of the active sites, possibly due to excessive coke deposition. The accelerated rate of deactivation at higher reaction temperatures offsets the increase in activity that would result with increasing temperature if coking and, as a result, diffusion limitations were not imposed.

An examination of the conversion profiles as a function of reaction time, illustrated in Fig. 3a, reveals a common shape for a wide range of activated zeolites. The presence of an initial induction period, which takes the form of increased relative conversions over the 0.5–1.5 h period, has also been observed for the dehydrogenation of cyclohexane and methylcyclohexane over the same catalysts (*36*). As in the case of the dehydrogenation reactions, this induction period can be explained on the basis of a stronger interaction of the product (in this case, ethylbenzene) relative to the reactants. As a result of this "hold-up" of ethylbenzene on the catalyst surface, the initial product samples exhibit a relative enrichment of the reactants, i.e., benzene and ethanol. The ethylation profiles for the acidic HY and CeKY were not characterized by such a marked increase in activity over the 0.5–1.5 h period, as can be seen in Fig. 3a. This is consistent with earlier infrared and chromatographic studies (*31, 35*) which suggested a higher relative freedom of movement of adsorbed aromatics of these surfaces. In the case of the HY and CeKY catalysts, which were initially the most active, the level of benzene conversion continued to decrease with time and the catalysts were rendered virtually inactive

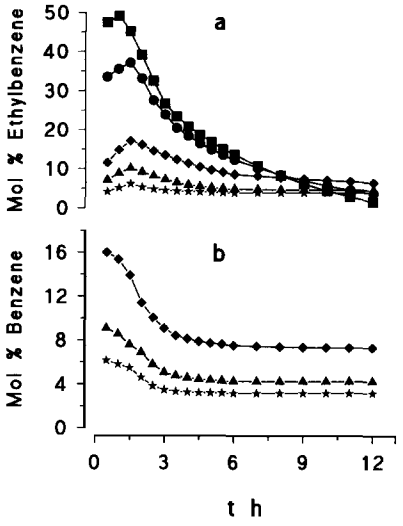

FIG. 3. Mol% conversion of (a) benzene to ethylbenzene and (b) cumene to benzene as a function of time-on-stream over samples of calcined HY (■) and CeKY-74.2 (●) and hydrogen-reduced NiLiY-43.1 (♦), NiNaY-35.7 (▲) and NiKY-49.1 (★) catalysts; $T_{reaction}$ = 573 K.

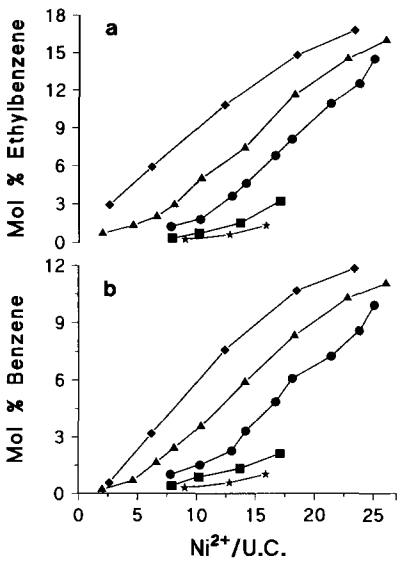

FIG. 4. Variation in mol % conversion of (a) benzene to ethylbenzene and (b) cumene to benzene (after 6 h on stream) as a function of nickel loading over a range of hydrogen-reduced NiLiY (♦), NiNaY (▲), NiKY (●), NiRbNaY (■), and NiCsNaY (★) catalysts.

after 12 h on stream. By comparison, all of the reduced nickel zeolites with metal loadings less than ca. 18 Ni^+/U.C. attained a steady state activity after 6 h on stream. There is thus a difference in behaviour with regard to catalyst activity between the acidic and dual functional surfaces.

Percentage mole conversion to ethylbenzene is plotted against nickel loading in Fig. 4a. On reduction, the higher loaded nickel catalysts exhibited the greater levels of ethylation. It may be observed that catalytic activity increases smoothly with nickel content over the range of NiLiY and NiNaY samples, whereas ethylbenzene formation only occurs at higher nickel loadings for the NiKY (>6 Ni^{2+}/U.C.) and NiRbNaY and NiCsNaY samples (>8 Ni^{2+}/U.C.). Data on the extent of Ni^{2+} reduction, the distribution of the hydroxyl groups within the zeolite framework, and the specific ethylation activities with regard the metal and acid functions are provided in Table 3. The degree of reduction of the exchanged divalent nickel cations is dependent on the level of nickel exchange and the nature of the alkali metal co-cation (*26, 31*). At low metal loadings, the more basic alkali metal counter-ions act to strengthen the coordination of Ni^{2+} to the zeolite lattice with the result that at metal loadings less than ca. 10 Ni^{2+}/U.C. the degree of reduction decreases in the order NiLiY > NiNaY > NiKY > NiRb NaY, NiCsNaY. At higher nickel concentrations, the higher level of surface acidity associated with the sodium and lithium-based catalysts inhibits the reduction process to a greater extent, yielding a reverse sequence of decreasing nickel cation reducibility at ca. 16 Ni^{2+}/U.C., i.e., NiCsNaY, NiRbNaY > NiKY > NiNaY > NiLiY. Indeed, it has been established in the literature (*37–40*) that the faujasite series shows a decrease in reduced nickel metal with increasing Brønsted acidity. Although the degree of Ni^{2+} reduction decreases with increasing metal loading, the number of protons generated (*24*) and the mass of supported metal (*27*) are higher and the specific ethylation activity at steady state is also greater (see Table 3). In general, as the nickel content is increased, the number of large-cage hydroxyl groups is increased with a resultant increase in the levels of conversion (see Fig. 4a and Table 3). However, the larger the alkali metal cocation, the greater is the tendency for protons to locate at inaccessible sites, which results in the lower observed ethylation activities for the NiRbNaY and NiCsNaY systems. The order of increasing ethylation, NiCsNaY < NiRbNaY < NiKY < NiNaY < NiLiY, is also that of the increasing ionic potential (and electron attracting ability) of the charge-balancing alkali metal co-cation. Therefore, in going from NiCsNaY to NiLiY, the greater the concentration of electrons in the neighbourhood of the alkali metal ion is (*41*). As the negative charge distribution is pulled towards the framework alkali ion, the electron cloud of the O–H bond will be drawn to the oxygen atom. Therefore, the larger the electron affinity of the alkali metal ion (Li^+

TABLE 3

The Influence of the Alkali Metal Counter-Ion on the Degree of Ni^{2+} Reduction, the Hydroxyl Group Distribution, and the Specific Ethylation Activity for a Range of Nickel-Loaded Y Zeolites: $T_{reaction}$ = 573 K; Benzene : Ethanol = 5 : 1

Zeolite sample	% Ni^{2+} Reduction[a]	L.C.[b] (H^+/U.C.)	S.C.[c] (H^+/U.C.)	Specific activity (h^{-1})	
				10^{-24} mol EB[d] (L.C. H^+)$^{-1}$	10^{-2} mol EB[e] (g Ni^0)$^{-1}$
HY	—	29.2	28.8	2.4	—
CeNaY-68.0	—	23.2	—	7.4	—
CeKY-74.2	—	24.7	—	7.5	—
NiLiY- 8.8	96	5.0	—	26.1	4.3
NiLiY-21.2	75	8.3	—	32.2	6.2
NiLiY-43.1	52	11.6	1.6	42.2	7.3
NiLiY-63.7	42	12.1	4.4	55.6	8.3
NiLiY-80.6	40	12.8	7.6	59.3	8.7
NiNaY-15.8	85	7.8	—	7.5	1.6
NiNaY-22.8	78	9.0	0.9	10.0	1.7
NiNaY-35.7	63	11.6	2.5	21.0	3.2
NiNaY-48.8	57	12.6	4.8	26.2	3.8
NiNaY-63.1	52	13.5	6.4	39.3	5.1
NiNaY-78.6	52	14.9	9.1	44.5	5.3
NiNaY-90.1	51	15.6	12.9	46.0	5.4
NiKY-26.9	64	3.1	7.5	17.2	1.3
NiKY-35.6	53	3.7	8.2	22.3	1.4
NiKY-49.1	56	7.7	10.5	26.9	1.9
NiKY-62.5	54	8.3	10.9	44.1	3.1
NiKY-73.8	53	10.6	13.0	47.4	3.7
NiKY-86.6	52	13.0	13.5	49.8	4.5
NiRbNaY-27.3	72	1.1	9.8	12.0	0.2
NiRbNaY-35.1	69	2.4	10.5	14.8	0.5
NiRbNaY-47.4	65	4.1	12.9	17.1	0.8
NiRbNaY-59.1	58	6.6	13.0	22.2	1.8
NiCsNaY-31.1	66	1.3	11.2	6.9	0.1
NiCsNaY-44.3	65	4.3	12.6	6.3	0.2
NiCsNaY-54.8	63	7.2	13.3	8.1	0.6
$NiNH_4Y$-8.5	3	24.4	28.8	3.2	88.3
$NiNH_4Y$-20.7	4	18.2	28.6	4.4	10.2
$NiNH_4Y$-52.2	2	4.1	24.4	24.2	13.3
$NiNH_4Y$-69.1	1	1.2	18.0	101.6	18.8

[a] From iodometric titrametric data (*26*).
[b] Number of large cage hydroxyl groups per unit cell (*24*).
[c] Number of small cage hydroxyl groups per unit cell (*24*).
[d] 10^{-24} moles of EB produced (per hour) per large cage Brønsted acid site.
[e] 10^{-2} moles of EB produced (per hour) per gram of supported nickel metal.

$> Na^+ > K^+ > Rb^+ > Cs^+$), the closer this electron cloud moves towards the lattice oxygen and the more positive is the hydrogen atom, weakening the surface O–H bond, making it more acidic and hence more reactive. As was reported for copper-exchanged Y zeolites (*42*), ethylation activity is essentially associated with Brønsted acid centres

TABLE 4

Effect of Pyridine Adsorption on the Specific Ethylation Activity at Steady State over a Range of Hydrogen-Reduced Nickel Zeolites: $T_{reaction}$ = 573 K; Benzene : Ethanol = 5 : 1

Zeolite sample	10^{-2} mol EB h^{-1} (g Ni^0)$^{-1}$	
	Untreated	Treated with pyridine
NiLiY-21.2	6.2	1.3
NiLiY-43.1	7.3	1.4
NiLiY-63.7	8.3	2.0
NiNaY-22.8	1.7	0.4
NiNaY-48.8	3.8	0.6
NiNaY-63.1	5.1	1.1
NiKY-49.1	1.9	0.4
NiKY-62.5	3.1	0.5
NiRbNaY-47.4	0.8	0.2
NiRbNaY-59.1	1.8	0.3
NiCsNaY-44.3	0.2	0.1
NiCsNaY-54.8	0.6	0.1

located in the accessible supercages. However, it has been shown (*43, 44*) that, at elevated temperatures, protons migrate from the small cages to the large cages. To develop this idea, a range of reduced nickel zeolites were treated with pyridine, which is effective in poisoning supercage hydroxyl groups (*24*), and should therefore render the catalyst inactive. As can be seen from the data presented in Table 4, the specific ethylation activity has been drastically reduced by the pyridine treatment, but there remains a residual activity which is similar for all the samples studied. Assuming that the pyridine treatment has been 100% effective in neutralizing the supercage acidity, the presence of any activity may be due to the migration of small cage "unpoisoned" protons into the supercage during catalysis.

The influence of the supported nickel metal phase on the activities exhibited by a range of reduced $NiNH_4Y$ catalysts is shown in Table 3. Although the nickel cations supported on NH_4Y should be more easily reduced from coordination considerations, the inhibiting effect of a high concentration of hydroxyl groups is overwhelming (*31*). Nevertheless, the protonic activity was markedly enhanced in the presence of trace quantities of supported nickel metal and increased with increasing metal content. While the number of large-cage protons (and hence the number of potential active sites) is lowered on exchanging NH_4^+ with Ni^{2+} ions (*24*), the overall effect of nickel exchange was to increase ethylbenzene formation. On the other hand, the incorporation of Ce^{3+} ions into the Y-zeolite lattice which has clearly been shown to result in the generation of additional Brønsted acidity (*24, 31*) also served to increase catalytic activity (Table 5) with increasing Ce^{3+}/Ni^{2+} ratios. There is, there-

TABLE 5

Effect of Ce^{3+} Exchange on the Specific Activity and Overall Levels of Ethylation at Steady State for a Range of Hydrogen-Reduced NiNaY and NiKY Zeolites: $T_{reaction}$ = 573 K; Benzene : Ethanol = 5 : 1

Zeolite sample	Ni^{2+}/Ce^{3+}	Mol% EB	Specific activity 10^{-2} mol EB h^{-1} (g Ni^0)$^{-1}$
CeNaY-68.0[a]	—	3.4	—
CeKY-74.2[a]	—	3.8	—
NiNaY-21.8[b]	—	2.1	1.8
CeNiNaY-21.6[b]	2.9	3.0	3.7
CeNiNaY-21.1	0.8	8.9	16.3
CeNiNaY-20.8	0.6	10.7	35.7
NiNaY-58.0	—	10.1	4.8
CeNiNaY-54.4	6.7	11.4	7.5
CeNiNaY-34.9	1.4	19.9	33.2
CeNiNaY-24.0	0.6	26.8	115.5
NiKY-25.0	—	1.0	1.2
CeNiKY-24.8	4.2	1.4	1.6
CeNiKY-24.3	0.9	4.6	6.6
CeNiKY-23.9	0.6	8.1	11.7
NiKY-56.9	—	6.0	2.4
CeNiKY-55.2	7.3	7.3	3.5
CeNiKY-48.8	2.1	12.3	8.1
CeNiKY-35.7	1.2	16.7	20.7

[a] Ce^{3+} loading.
[b] Ni^{2+} loading.

fore, a fine interweaving of the acidic activities and the promotional effect of the "inert" metal which ultimately leads to a maximum level of ethylation activity.

From these observations, it can be stated that a catalyst pretreatment which results in higher levels of Ni^{2+} reduction in the catalyst precursor and, in turn, a greater concentration of surface acid sites serves to promote the level of steady-state ethylation. For example, the introduction of an N_2-pretreatment step prior to hydrogen reduction which has been reported to diminish the degree of cation reduction (*26*) also inhibits the extent of surface hydroxyl formation (*24*). Taking the NiLiY-43.1 catalyst as a representative case, the introduction of a precalcination step lowered the specific ethylation activity from 7.3×10^{-2} to 5.9×10^{-2} mol EB h^{-1} (g $Ni^0)^{-1}$. In complete contrast, the treatment of NiNaY and NiKY samples with NaOH and KOH solutions, which brings about a considerable enhancement of nickel cation reduction (*45*), results in improved ethylation specific activities, e.g., treatment of NiNaY-63.1 with an aqueous NaOH solution (pH = 13) raised the specific activity from 5.1×10^{-2} to 5.9×10^{-2} mol EB h^{-1} (g $Ni^0)^{-1}$.

Reduction of the nickel zeolites prepared by impregnation generated negligible surface acidity (*24*) and consequently the level of ethylbenzene formation was considerably lower than that recorded for the ion-exchanged catalysts; the actual values were similar to those obtained over calcined NiY catalysts. Although the impregnated Ni/SiO_2 and Ni/Al_2O_3 precursors exhibit a higher degree of Ni^{2+} cation reduction when compared with the Y zeolites (under the same reduction conditions) (*31*), the levels of ethylation are much lower over the amorphous supports (see Table 6). This is not surprising in view of the fact that the Brønsted acid strengths of the silica and alumina carriers are lower and the number of supported acid sites is much greater for HY (*46*). In addition, the spatial distribution of oxygen atoms in the Y-zeolite framework must also facilitate a greater interaction of the reactant molecules with the surface hydroxyl groups.

TABLE 6

The Effect of the Support on the Steady-State Specific Ethylation Activity: $T_{reaction}$ = 573 K; Benzene : Ethanol = 5 : 1

Nickel catalyst	% w/w Ni	10^{-2} moles EB h^{-1} (g $Ni^0)^{-1}$
NiNaY-22.8[a]	2.4	1.7
Ni/SiO_2	2.8	0.2
Ni/Al_2O_3	2.2	0.4
NiNaY-48.8[b]	4.6	3.8
Ni/SiO_2	4.8	0.3
Ni/Al_2O_3	4.3	0.7
NiNaY-90.1[c]	8.6	5.4
Ni/SiO_2	9.7	0.5
Ni/Al_2O_3	9.2	0.9

[a] 6.6 Ni^{2+}/U.C.
[b] 14.1 Ni^{2+}/U.C.
[c] 26.1 Ni^{2+}/U.C.

For a particular catalyst to be commercially viable it is essential that it can be used repeatedly without any appreciable loss of catalytic activity. In the case of the lower loaded (<14 Ni^{2+}/U.C.) nickel zeolites, activity was recoverable by flushing the spent catalysts in purified hydrogen (150 cm^3 min^{-1}) for 12 h at 723 K. This was not possible for the higher loaded nickel catalysts, which exhibited an irreversible deactivation (see Table 7), resulting in the complete loss of activity after four reaction cycles. Deactivation of zeolites normally results from the generation of large coke molecules within the pore structure which are too large to diffuse out and so remain entrapped within the zeolite channels. To test whether coke deposition was operative in this particular catalytic system, the residual carbon contents of a number of spent catalysts was measured and the resultant data are plotted against nickel loading in Fig. 5. The carbon content of the NiRbNaY and NiCsNaY samples was negligible. The amount of car-

TABLE 7

Effect of Oxidative Regeneration on the Level of Benzene Ethylation (after 6 h on Stream) over Three Selected Zeolites: $T_{reaction}$ = 573 K; Benzene: Ethanol = 5 : 1

Catalytic reaction	Mol% ethylbenzene		
	NiLiY-63.7	NiKY-62.5	NiCsNaY-54.8
Reaction 1	14.1	8.2	3.6
Reaction 2	5.2	5.9	3.0
Reaction 3	0.3	3.8	2.2
Regeneration 1	12.1	8.0	3.5
Regeneration 2	10.9	7.1	3.3
Regeneration 3	9.2	6.6	3.0
Regeneration 6	6.4	5.3	2.4
Regeneration 10	1.9	3.2	1.7

bon deposited on the spent NiLiY, NiNaY, and NiKY catalysts increased with increasing nickel loading and the order of increasing coke content, at each level of nickel exchange, is NiCsNaY < NiRbNaY < NiKY < NiNaY < NiLiY. These values are much lower than those measured for samples of spent HY (21.5%) and CeKY-74.2 (19.3%). Catalyst deactivation must therefore result from the gradual accumulation of involatile coke species in the zeolite channels. The stabilizing effect of the supported metal phase may stem from an ability to hydrogenate or dehydrogenate any coke precursors thereby inhibiting the laydown of critical amounts of coke. The most common industrial procedure for reclaiming spent catalysts is simply to oxidise the coke to carbon oxides and water in a stream of oxygen at temperatures of 673–773 K (*47, 48*). As can be seen from the data presented in Table 7, the oxidative regeneration of the deactivated nickel catalysts was successful in restoring ethylation activity. On resuming catalysis without further regeneration the level of ethylbenzene formation again dropped. In any case, the catalysts exhibited minimal activity after 10 regeneration cycles.

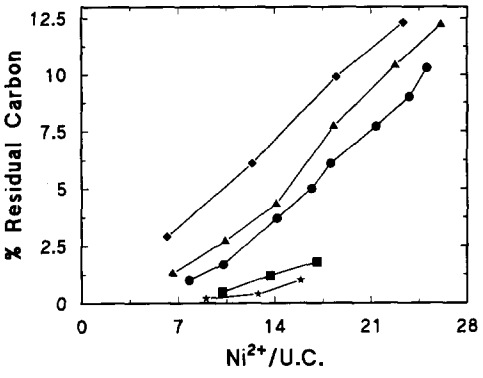

FIG. 5. The variation in coke deposition during the ethylation of benzene as a function of nickel exchange over a range of hydrogen-reduced NiLiY (♦), NiNaY (▲), NiKY (●), NiRbNaY (■),and NiCsNaY (★) catalysts.

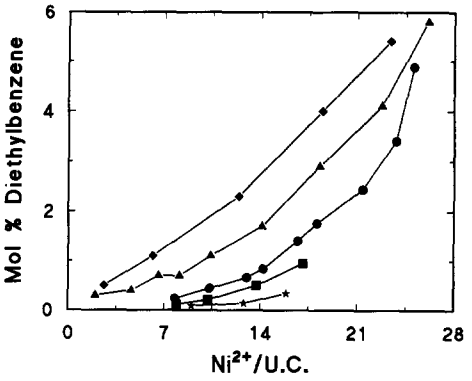

FIG. 6. Variation in mol% conversion to diethylbenzenes (*meta-* + *para-* + *ortho*-isomers) at 573 K, as a function of nickel exchange over a range of hydrogen-reduced NiLiY (♦), NiNaY (▲), NiKY (●), NiRbNaY (■), and NiCsNaY (★) catalysts.

Catalysis over the more active samples resulted in the formation of diethylbenzenes (DEB). The extent of DEB formation is plotted against nickel loading in Fig. 6. As expected, the level of DEB production was highest over the most acidic samples and at a metal loading of ca. 10 Ni^{2+}/U.C. increased in the order NiCsNaY < NiRbNaY < NiKY < NiNaY < NiLiY. The three isomers (*meta-*, *ortho-*, and *para-*) of DEB were isolated in the product mixture. The distribution of each of the isomers as a function of nickel content for the NiLiY, NiKY, and NiRbNaY systems is illustrated in Fig.

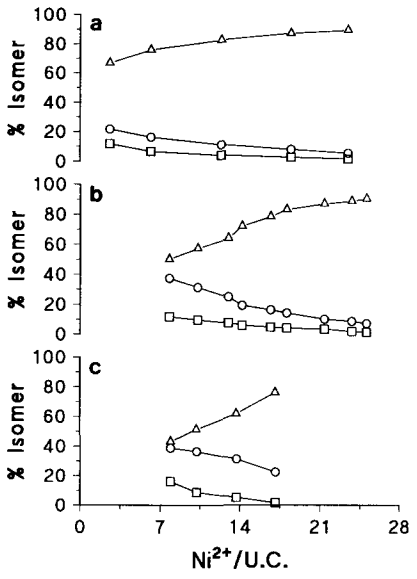

FIG. 7. Diethylbenzene isomer distribution resulting from the ethylation of benzene at 573 K over a range of hydrogen-reduced (a) NiLiY, (b) NiKY, and (c) NiRbNaY catalysts: *para*-isomer (△); *meta*-isomer (□); *ortho*-isomer (○).

7. It is clear that the relative quantity of each isomer is dependent on the nature of the alkali metal co-cation; in the presence of the larger Rb^+ (and Cs^+) cations the *ortho*-isomer is promoted to a greater extent than is the case for the LiY, NaY, and KY supports. The NiLiY and NiNaY catalysts exhibited a higher selectivity for *para*-isomer formation, whereas the fraction of the *meta*-isomer in the product is essentially independent of the co-cation. As the nickel content is increased, *para*-DEB is preferentially formed at the expense of the *ortho*-form, regardless of the support. *Para*-isomer production is therefore promoted with increasing surface acidity and follows the sequence NiCsNaY < NiRbNaY < NiKY < NiNaY < NiLiY. As has been suggested from previous studies (*3, 4, 6*), this increased *para*-selectivity can be related to an increased level of occluded coke deposition (Fig. 5) which serves to decrease the intracrystalline channel diameters, thereby introducing a configurational diffusion limitation.

Cumene Dealkylation

Cumene conversion over the range of catalysts considered in this study resulted only in the formation of benzene and propylene. As in the case of benzene ethylation, the extent of cumene dealkylation increased with increasing reaction temperature in the range 473–623 K, as illustrated in Fig. 2b. The flattening of the curves at temperatures greater than ca. 573 K can again be attributed to coke depositions which impose diffusion restraints on the reaction. Representative conversion vs time on stream profiles are shown in Fig. 3b. As cumene interacts more strongly with the zeolite surface than does benzene (*31*), the initial induction period observed for the ethylation reaction is not manifest in this instance. The levels of cracking over the metal-loaded zeolites reach equilibrium after 6 h on stream, whereas the fully decationized HY zeolite exhibits negligible activity after extended use.

The dependence of cumene conversion on nickel loading, illustrated in Fig. 4b and Table 8, follows the same trends observed for benzene ethylation. Catalytic cumene cracking activity also increases in the order NiCsNaY < NiRbNaY < NiKY < NiNaY < NiLiY. However, the levels of specific

TABLE 8

Specific Dealkylation Activity at Steady State and the Residual Carbon Contents (after 6 h on Stream) of a Range of Activated Y Zeolites: $T_{reaction}$ = 573 K; W/F = 83.3 g mol^{-1} h

Zeolite sample	Specific activity h^{-1}		% Residual carbon
	10^{-24} mol C_6H_6 (L.C. $H^+)^{-1}$	10^{-4} mol C_6H_6 (g $Ni^0)^{-1}$	
HY	2.0	—	16.2
CeKY-74.2	5.3	—	11.4
NiLiY-43.1	23.5	4.1	8.9
NiLiY-80.6	33.3	4.7	10.6
NiNaY-48.8	16.8	2.5	6.7
NiNaY-78.6	24.8	3.0	9.2
NiKY-49.1	15.0	1.1	5.4
NiKY-82.0	23.8	2.1	8.5
NiRbNaY-59.1	11.6	0.8	4.3
NiCsNaY-54.8	5.1	0.4	3.2

activity are lower than those observed for the ethylation reaction (see Table 3). This may suggest that stronger acid sites are required to promote cumene dealkylation. The role of the supported nickel metal in promoting the protonic activity is also operable during cumene cracking and the specific activities measured for the nickel-loaded catalysts are higher than those recorded for the ammonium and cerium exchanged forms (see Table 8). In addition, the carbon contents (and hence the level of coking) of a range of spent samples were measured and are also included in Table 8. The more acidic catalysts exhibited the highest carbon contents; the presence of nickel metal on the support again inhibits the deposition of large amounts of coke as can be inferred from the smaller residual carbon contents of the NiY zeolites.

CONCLUSIONS

The specific effect of the alkali metal cocation on the siting of hydroxyl groups within the zeolite framework, the surface acid strength, and the nature of the supported nickel phase translates into the observed protonic activities. While the zeolitic Brønsted acid sites are the active centres for the ethylation of benzene and dealkylation of cumene, the presence of nickel metal on the support prolongs the catalyst lifetime and generates a higher level of ethylation/cracking at steady state. This effect is presumably due to the conversion of any coke precursors, with the result that the levels of coke deposition are lowered and the intracrystalline active sites remain accessible to the incoming reactant molecules. In contrast, the (initially) more active HY and CeY samples deactivate continuously with time. An optimum in steady-state protonic activity can be achieved by a "fine-tuning" of the acid and metal functions of the catalyst. Benzene was converted to diethylbenzenes over the higher nickel loaded zeolites. While the *para*-DEB isomer was preferred over the entire range of catalysts studied, a distinctly higher fractional conversion to the *ortho*-isomer was observed for the NiRb NaY and NiCsNaY systems. Catalyst deactivation resulted from the deposition of coke within the zeolite pores, which restricted access of the reactants to the Brønsted acid sites. Regeneration of the deactivated catalysts by burning off the coke in a stream of oxygen restored activity, but prolonged regeneration ultimately results in the irreversible deactivation of the catalysts.

REFERENCES

1. Jacobs, P. A., "Carboniogenic Activity of Zeolites." Elsevier, Amsterdam, 1977.
2. Barthomeuf, D., *J. Phys. Chem.* **83,** 249 (1979).
3. O'Donoghue, E., Ph.D thesis, National University of Ireland, 1983.
4. Nunan, J., Ph.D thesis, National University of Ireland, 1981.
5. Venuto, P. B., *Adv. Chem. Ser.* **102,** 260 (1971).
6. Coughlan, B., Carroll, W. M., and Nunan, J., *J. Chem. Soc. Faraday Trans. 1* **79,** 281 (1983).
7. Mukheryer, P. N., and Basu, P. K., *Chem. Age India* **33,** 202 (1982).
8. Ollis, D. F., *J. Catal.* **23,** 131 (1971).
9. Liengme, B. V., and Hall, K. W., *Trans. Faraday oc.* **62,** 3229 (1966).
10. Pickert, B. E., Bolton, A. B., and Lanewala, M. A., *Chem. Eng. Prog. Symp. Ser.* **63,** 50 (1967).
11. Becker, K. A., Karge, H. G., and Streubel, W. D., *J. Catal.* **28,** 403 (1973).
12. Yashima, T., Ahmod, H., Yamazaki, K., Katsuata, M., and Hara, N., *J. Catal.* **17,** 151 (1970).
13. Yashima, T., Sato, K., Hayaska, T., and Hara, N., *J. Catal.* **26,** 303 (1972).
14. Selfick, M. D., *J. Am. Chem. Soc.* **101,** 2164 (1979).
15. Igarashi, T., Takahashi, H., and Suzuki, M., *Rep. Fac. Eng. Kanagawa Univ.* **22,** 22 (1984).
16. King, S. T., and Graces, J. M., *J. Catal.* **104,** 59 (1987).
17. Engelhardt, J., Szanyi, J., and Valyon, J., *J. Catal.* **107,** 296 (1987).
18. Itoh, H., Hattori, T., Suzuki, K., and Murakami, Y., *J. Catal.* **79,** 21 (1983).
19. Venuto, P. B., and Landis, P. S., *in* "Advances in Catalysis" (D. D. Eley, H. Pines, and P. B. Weisz, Eds), Vol. 18, p. 259. Academic Press, New York, 1968.
20. Richardson, J. T., *J. Catal.* **9,** 182 (1967).
21. Hatcher W. J., *Ind. Eng. Chem. Prod. Res. Dev.* **24,** 10 (1985).
22. Rabo, J. A., and Poutsma, M. L., *Am. Chem. Soc. Symp. Ser.* **42,** 284 (1978).
23. Tsutsumi, K., Fuji, S., and Takahashi, H., *J. Catal.* **24,** 8 (1972).
24. Coughlan, B., and Keane, M. A., *J. Colloid. Interface Sci.* **137,** 483 (1990).

25. McDaniel, C. V., and Maher, P. K., *Am. Chem. Soc. Monogr.* **121,** 285 (1976).
26. Coughlan, B., and Keane, M. A., *J. Catal.* **123,** 364 (1990).
27. Coughlan, B., and Keane, M. A., *Zeolites* **11,** 2 (1991).
28. Flanigen, E. M., Khatami, H., and Szymauski, H. A., *Adv. Chem. Ser.* **101,** 201 (1971).
29. Coughlan, B., and Keane, M. A., *Zeolites* **11,** 12 (1991).
30. Vogel, A., "Practical Organic Chemistry." Longmans, London, 1978.
31. Keane, M. A., Ph.D thesis, Vol. 1 and 2, National University of Ireland, 1988.
32. Coughlan, B., and Keane, M. A., *Catal. Lett.* **5,** 101 (1990).
33. Coughlan, B., and Keane, M. A., *J. Mol. Catal.* **71,** 93 (1992).
34. Coughlan, B., and Keane, M. A., *Zeolites* **11,** 489 (1991).
35. Coughlan, B., and Keane, M. A., *J. Chem. Soc. Faraday Trans.* **86,** 3961 (1990).
36. Coughlan, B., and Keane, M. A., *Catal. Lett.* **5,** 89 (1990).
37. Richardson, J. T., *J. Catal.* **21,** 122 (1971).
38. Suzuki, M., Tsutsumi, K., and Takahashi, H., *Zeolites* **2,** 51 (1982).
39. Garbowski, E., Mirodatos, C. and Primet, M., *Stud. Surf. Sci. Catal.* **12,** 235 (1982).
40. Exner, D., Jaeger, N. I., Nowak, R., Schulz-Ekloff, G., and Ryder, P., *in* "Proceedings of the 6th International Zeolite Conference" (D. Olson and A. Bisio, Eds.), p. 387, Butterworths, London, 1984.
41. Richardson, J. T., *J. Catal.* **32,** 275 (1968).
42. Coughlan, B., and Keane, M. A., *Catal. Lett.* **5,** 11 (1990).
43. Beaumont, R., and Barthomeuf, D., *J. Catal.* **27,** 45 (1972).
44. Freude, D., Oehme, W., Schmeidel, H., and Staudte, B., *J. Catal.* **27,** 45 (1974).
45. Coughlan, B., and Keane, M. A., *J. Mol. Catal.* **63,** 193 (1990).
46. Fraissard, J., *Stud. Surf. Sci. Catal.* **5,** 343 (1980).
47. Ellingham, R. E., and Garret, J., *Appl. Ind. Catal.* **3,** 25 (1984).
48. Pennline, H. W., and Pollack, S. S., *Ind. Eng. Chem. Prod. Res. Dev.* **25,** 11 (1986).